

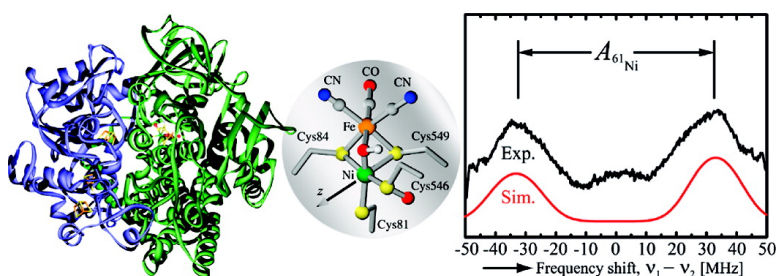
Communication

Electron–Electron Double Resonance-Detected NMR to Measure Metal Hyperfine Interactions: Ni in the Ni–B State of the [NiFe] Hydrogenase of *Desulfovibrio vulgaris* Miyazaki F

Marco Flores, Aruna Goenka Agrawal, Maurice van Gastel, Wolfgang Grtner, and Wolfgang Lubitz

J. Am. Chem. Soc., **2008**, 130 (8), 2402-2403 • DOI: 10.1021/ja077976x

Downloaded from <http://pubs.acs.org> on February 8, 2009



More About This Article

Additional resources and features associated with this article are available within the HTML version:

- Supporting Information
- Access to high resolution figures
- Links to articles and content related to this article
- Copyright permission to reproduce figures and/or text from this article

[View the Full Text HTML](#)

Electron–Electron Double Resonance-Detected NMR to Measure Metal Hyperfine Interactions: ^{61}Ni in the Ni–B State of the [NiFe] Hydrogenase of *Desulfovibrio vulgaris* Miyazaki F

Marco Flores, Aruna Goenka Agrawal, Maurice van Gastel, Wolfgang Gärtner, and Wolfgang Lubitz*

Max-Planck-Institut für Bioanorganische Chemie, Stiftstrasse 34-36, D-45470 Mülheim an der Ruhr, Germany

Received October 17, 2007; E-mail: lubitz@mpi-muelheim.mpg.de

The electron–nuclear hyperfine couplings (hfc's) between the unpaired electron of the paramagnetic active site of a metalloprotein and magnetic nuclei provide information about the electronic and geometric structure of the active site, which are related to the function of the protein. Electron–nuclear double resonance (ENDOR) spectroscopy^{1,2} is the method of choice to resolve the hfc and the nuclear quadrupole coupling (nqc) but is limited in certain cases by fast electron and/or nuclear relaxation.² For this reason the ENDOR detection of the central metal has only been described for a few cases.³ With the advent of electron–electron double resonance-detected NMR (EDNMR),^{2,4} a new hyperfine resolving technique has become available, which does not employ radio frequency (rf) pulses to excite NMR transitions. Here, we demonstrate the usefulness of EDNMR for measuring metal hyperfine interactions of active sites in metalloproteins using [NiFe] hydrogenase as an example.

In the EDNMR experiment, three microwave (MW) pulses are applied to the system (Scheme 1). The first MW pulse, with a variable frequency ν_1 excites electron paramagnetic resonance (EPR) forbidden transitions (see Supporting Information). The second and third MW pulses are the detection pulses, which give rise to the Hahn echo at a fixed frequency ν_2 . Nuclear magnetic transitions are excited when the first pulse is resonant with an EPR forbidden transition (at ν_1) while detecting an EPR allowed transition (at ν_2).⁴ Thus, EDNMR spectra are plots of the EPR signal amplitude versus the shift between the two MW frequencies ($\nu_1 - \nu_2$). So far, this technique has been applied successfully to detect ^{55}Mn resonances in photosystem II.⁵ For metals, in particular for ^{61}Ni ($I = 3/2$), the EDNMR signal could be more intense than the ENDOR signal. This is related to the fact that all EPR transitions of the system ($S = 1/2$, $I = 3/2$) become allowed to some extent, because dipolar and nuclear quadrupole couplings cause the nuclear eigenstates of both M_S manifolds to be slightly different. For a system with a dominant hfc interaction (A) the EDNMR signals occur when $\nu_1 - \nu_2$ is approximately equal to $\pm A/2$, $\pm A$, or $\pm 3A/2$. In this work EDNMR at Q-band (34 GHz) was used to measure the hfc's of ^{61}Ni in the Ni–B state of the [NiFe] hydrogenase from *Desulfovibrio* (*D.*) *vulgaris* Miyazaki F. This enzyme catalyzes the reversible oxidation of H_2 (reviewed in ref 6).

Figure 1 shows the active site of the enzyme, which contains the NiFe center and its ligands. In the oxidized state a third ligand bridging Ni and Fe is present.^{7,9} For the Ni–B state, this ligand was identified as OH^- using single-crystal ENDOR and density functional theory (DFT).⁸ The nickel is five-coordinate, the free coordination site is believed to serve as the contact position for dihydrogen in the catalytic process. Information about the electronic structure of the nickel is best obtained from the metal hfc and nqc tensors which require ^{61}Ni labeling of the enzyme and application of a suitable method to resolve these interactions. ^{61}Ni enrichment

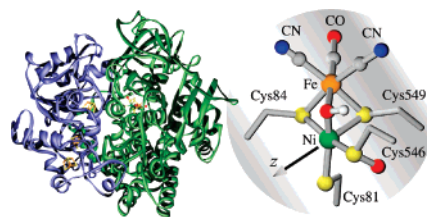
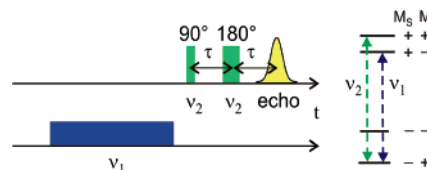


Figure 1. Structure of the [NiFe] hydrogenase from *Desulfovibrio vulgaris* Miyazaki F (left). Active site showing the NiFe center with ligand sphere,⁷ including $\text{X} = \text{OH}^-$ as bridging ligand⁸ for Ni–B (right) (modified from Brookhaven Data Bank entry 1WUJ).

Scheme 1. EDNMR Pulse Sequence and Energy Level Diagram ($S = 1/2$, $I = 1/2$) with Allowed and Forbidden Transitions ($|A/2| > \nu_n$)



has been used earlier to unambiguously detect the presence of nickel in this class of enzymes.^{10,11} Since ^{61}Ni ENDOR signals could not be detected, we used EDNMR, applied at Q-band frequencies to increase the spectral sensitivity and the (nuclear) Zeeman resolution, to measure the hyperfine interaction.

To enrich the protein with ^{61}Ni , cell cultures were grown using a minimal medium,¹² in which $10 \mu\text{M}$ of $^{61}\text{NiCl}_2$ was added. The enrichment was checked by EPR to be more than 90%. Ni–B was prepared as described.⁷ Figure 2a shows the electron spin echo (ESE) detected EPR spectrum of the Ni–B state. The observed g -values ($g_x = 2.33$, $g_y = 2.16$, $g_z = 2.01$) are in agreement with those reported previously.¹³ Figure 2b shows the EDNMR spectra of Ni–B samples, with and without ^{61}Ni enrichment, recorded at the field position B_5 (Figure 2a). In the non-enriched sample, the signal at 0 MHz is due to the allowed EPR transition, and the sharp lines at ± 50 MHz belong to ^1H resonances. These signals are also present in the ^{61}Ni enriched sample. The arrows in Figure 2b indicate the positions of ^{61}Ni EDNMR signals that are best observed in the spectrum of the enriched sample. They correspond to nuclear magnetic transitions around $\pm A/2$, $\pm A$, and $\pm 3A/2$ with shifts of about ± 25 , ± 50 , and ± 75 MHz, respectively, at this field position. The signals around ± 50 MHz overlap with those corresponding to ^1H . Figure 2c shows difference ($^{58/60}\text{Ni} - ^{61}\text{Ni}$) EDNMR spectra recorded at different magnetic field positions within the ESE detected EPR spectrum (B_1, \dots, B_7 in Figure 2a), along which molecules with a particular set of directions were selected.¹⁴ The difference spectra contain only ^{61}Ni EDNMR signals. The principal components of the ^{61}Ni hfc tensor were assumed to have the same sign. Negative values are expected due to the negative sign of the ^{61}Ni gyromagnetic ratio. This is confirmed by theoretical calcula-

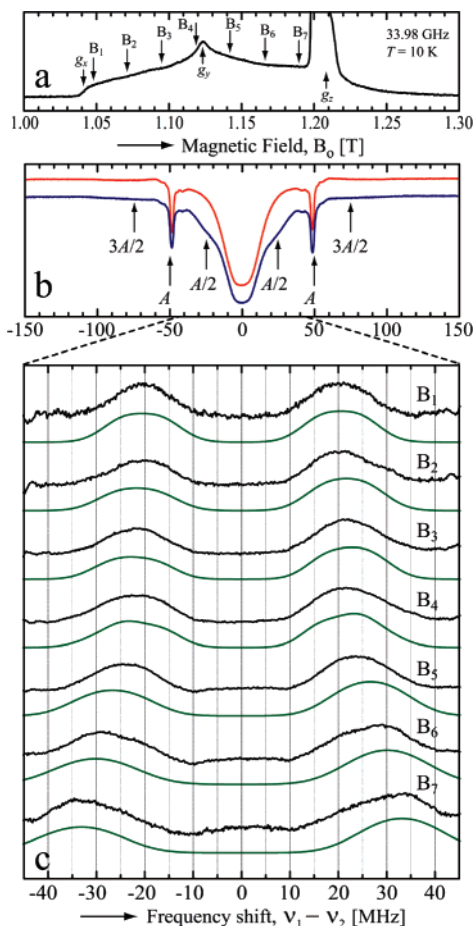


Figure 2. (a) Q-band ESE detected EPR spectrum of Ni–B in the [NiFe] hydrogenase from *D. vulgaris* Miyazaki F. The signal between 1.20 and 1.22 T corresponds to the [3Fe4S] cluster. EDNMR spectra were recorded at the field positions (B_1 , ..., B_7) indicated by arrows. (b) EDNMR spectra of $^{58/60}\text{Ni}$ (natural abundance, $I = 0$, red) and ^{61}Ni (enriched, $I = 3/2$, blue) samples recorded at 1.142 T (B_5). (c) Experimental (black) and simulated (green) difference ($^{58/60}\text{Ni} - ^{61}\text{Ni}$) EDNMR spectra, recorded at different magnetic field positions (B_1 , ..., B_7). These spectra show only the signals around $\pm A/2$. Experimental conditions: Sample concentration ≈ 1 mM, sample volume = 30 μL , $T = 10$ K, $\nu_2 = 33.98$ GHz, $\tau_{\text{ELDOR}} = 90$ μs (ν_1), detection pulses 160 and 320 ns (ν_2). Total averaging time per spectrum was about 20 min.

tions of the hfc's.¹⁵ The analysis of the EDNMR spectra by computer simulations^{16,17} yielded both the principal components of the hfc tensor ($A_x = -41$ MHz, $A_y = -38$ MHz, $A_z = -71$ MHz) and its orientation (i.e., Euler angles) with respect to the principal axes of the g-tensor of Ni–B, whose orientation with respect to the structure of the active site is known from single-crystal EPR experiments.¹³ The values for the hfc tensor are in agreement with those obtained independently from simulations of the EPR spectra. However, EDNMR retains the high resolution of the ^{61}Ni hfc where EPR is poorly resolved. Furthermore, magnitude and orientation of the hfc tensor obtained from the new method are more accurate than those obtained from EPR (see Supporting Information). The nqc is not resolved in the spectra, but contributes to the EDNMR line width.

The hfc tensor yields an isotropic hfc (A_{iso}) of -50 MHz and anisotropic couplings of (+9, +12, -21 MHz) for Ni–B. Using second-order crystal field theory for single d-electrons (see Table 1 in ref 18) and assuming Ni(III) for Ni–B with $3d^2$ as the ground

state,⁶ the spin population at ^{61}Ni can be estimated to be 0.44. This result is consistent with previous DFT estimations, which gave 0.52.¹⁹ The distribution of the remaining spin density over the ligands¹⁹ may be responsible for the significant deviation of the ^{61}Ni anisotropic couplings from axial symmetry and the observed slight deviation of the hfc and g tensors axes (see Supporting Information). This shows that the ligand sphere fine-tunes the electron density at the active site.

This work represents the first determination of a complete ^{61}Ni hfc tensor in hydrogenase research and shows that the EDNMR technique is a powerful method to elucidate metal hfc tensors in cases where ENDOR spectroscopy is difficult to perform. It should be applicable also to other paramagnetic states of [NiFe] hydrogenases.⁶ Such experiments are in progress in our laboratory to obtain the ^{61}Ni hfc tensors of all states.

Acknowledgment. We thank Tanja Berndsen for technical assistance and Hideaki Ogata for helping to prepare the enzyme in a pure Ni–B redox state. This work was supported by the Max-Planck-Gesellschaft and EU (SOLAR-H).

Supporting Information Available: Spin Hamiltonian for a system $S = 1/2$, $I = 3/2$; definition of NMR, EPR forbidden and EPR allowed transitions; fit of continuous wave EPR spectra. This material is available free of charge via the Internet at <http://pubs.acs.org>.

References

- (1) Feher, G. *Phys. Rev.* **1956**, *103*, 834–835.
- (2) Schweiger, A.; Jeschke, G. *Principles of Pulse Electron Paramagnetic Resonance*; Oxford University Press: Oxford, U.K., 2001.
- (3) Fan, C.; Gorst, C. M.; Ragsdale, S. W.; Hoffman, B. M. *Biochemistry* **1991**, *30*, 431–435. Gurbel, R. J.; Fann, Y. C.; Surerus, K. K.; Werst, M. M.; Musser, S. M.; Doan, P. E.; Chan, S. I.; Fee, J. A.; Hoffman, B. M. *J. Am. Chem. Soc.* **1993**, *115*, 10888–10894. Pelouquin, J. M.; Campbell, K. A.; Britt, R. D. *J. Am. Chem. Soc.* **1998**, *120*, 6840–6841. Harmer, J.; Finazzo, C.; Piskorski, R.; Bauer, C.; Jaun, B.; Duin, E. C.; Goenrich, M.; Thauer, R. K.; van Doorslaer, S.; Schweiger, A. *J. Am. Chem. Soc.* **2005**, *127*, 17744–17755. Silakov, A.; Reijerse, E. J.; Albracht, S. P. J.; Hatchikian, E. C.; Lubitz, W. *J. Am. Chem. Soc.* **2007**, *129*, 11447–11458. Kulik, L. V.; Epel, B.; Lubitz, W.; Messinger, J. *J. Am. Chem. Soc.* **2007**, *129*, 13421–13435.
- (4) Schosseler, P.; Wacker, T.; Schweiger, A. *Chem. Phys. Lett.* **1993**, *224*, 319–324.
- (5) Mino, H.; Ono, T. *Appl. Magn. Reson.* **2003**, *23*, 571–583. Kulik, L.; Epel, B.; Messinger, J.; Lubitz, W. *Photosynth. Res.* **2005**, *84*, 347–353.
- (6) Lubitz, W.; Reijerse, E.; van Gestel, M. *Chem. Rev.* **2007**, *107*, 4331–4365.
- (7) Ogata, H.; Hirota, S.; Nakahara, A.; Komori, H.; Shibata, N.; Kato, T.; Kano, K.; Higuchi, Y. *Structure* **2005**, *13*, 1635–1642.
- (8) van Gestel, M.; Stein, M.; Brecht, M.; Schröder, O.; Lendzian, F.; Bittl, R.; Ogata, H.; Higuchi, Y.; Lubitz, W. *J. Biol. Inorg. Chem.* **2006**, *11*, 41–51.
- (9) Volbeda, A.; Martin, L.; Cavazza, C.; Matho, M.; Faber, B. W.; Roseboom, W.; Albracht, S. P. J.; Garcin, E.; Rousset, M.; Fontecilla-Camps, J. C. *J. Biol. Inorg. Chem.* **2005**, *10*, 239–249.
- (10) Albracht, S. P. J.; Graf, E. G.; Thauer, R. K. *FEBS Lett.* **1982**, *140*, 311–313.
- (11) Moura, J. J. G.; Moura, I.; Huynh, B. H.; Krüger, H. J.; Teixeira, M.; DuVarney, R. C.; DerVartanian, D. V.; Xavier, A. V.; Peck, H. D.; LeGall, J. *Biochem. Biophys. Res. Commun.* **1982**, *108*, 1388–1393.
- (12) Goenka Agrawal, A.; van Gestel, M.; Gärtner, W.; Lubitz, W. *J. Phys. Chem. B.* **2006**, *110*, 8142–8150.
- (13) Trofanchuk, O.; Stein, M.; Gessner, C.; Lendzian, F.; Higuchi, Y.; Lubitz, W. *J. Biol. Inorg. Chem.* **2000**, *5*, 36–44.
- (14) Rist, G. H.; Hyde J. S. *J. Chem. Phys.* **1968**, *49*, 2449–2451.
- (15) Stein, M.; Lubitz, W. *J. Inorg. Biochem.* **2004**, *98*, 862–877.
- (16) EDNMR signals at $\pm A/2$ occur at frequencies values similar to those expected in ENDOR (see Supporting Information). Thus, EDNMR spectra (see Figure 2c) were simulated using ENDOR frequencies obtained by diagonalization of the spin Hamiltonian. The fitting procedure was that described in ref 17.
- (17) Flores, M.; Isaacson, R.; Abresch, E.; Calvo, R.; Lubitz, W.; Feher, G. *Biophys. J.* **2007**, *92*, 671–682.
- (18) Rieger, P. H. *Coord. Chem. Rev.* **1994**, *135/136*, 203–286.
- (19) Stein, M.; Lubitz, W. *Phys. Chem. Chem. Phys.* **2001**, *3*, 2668–2675.

JA077976X